# NetShaper: A Differentially Private Network Side-Channel Mitigation System

*(Confidential, please do not circulate!)*


## Abstract

The widespread adoption of encryption in network protocols has significantly improved the overall security of many Internet applications. However, these protocols cannot prevent *network side-channel leaks*—leaks of sensitive information through the sizes and timing of network packets. We present NetShaper, a system that mitigates such leaks based on the principle of traffic shaping. NetShaper's traffic shaping provides differential privacy guarantees while adapting to the prevailing workload and congestion condition, and allows configuring a tradeoff between privacy guarantees, bandwidth and latency overheads. Furthermore, NetShaper provides a modular and portable tunnel endpoint design that can support diverse applications. We present a middlebox-based implementation of NetShaper and demonstrate its applicability in a video streaming and a web service application.


## 1 Introduction

With the proliferation of TLS and VPN, traffic encryption has become the de facto standard for securing data in transit in Internet applications. Traffic can be encrypted at various layers, such as HTTPS, QUIC, and IPSec. While these protocols prevent *direct* data breaches on the Internet, they cannot prevent leaks through *indirect* observations of the encrypted traffic.

Indeed, encryption cannot conceal the shape of an application's traffic, i.e., the sizes, timing, and number of packets sent and received by an application. In many applications, these parameters strongly correlate with sensitive information. For instance, traffic shape can reveal video streams [43], website visits [8, 55], the content of VoIP conversations [58], and even users' medical and financial secrets [13].

In such *network side-channel leaks*, an adversary (e.g., a malicious or a compromised ISP) observes the shape of an application's traffic as it passes through a link under its control and infers the application's sensitive data from this shape.

Obfuscation techniques, which add ad hoc noise [33] or adversarial noise [37, 40, 44] in an application's network traces, do not provide comprehensive protection against network side-channel attacks [63]. In fact, recent advances in machine learning (ML) have greatly improved the ability to filter out noise due to congestion or path variations and infer secrets from noisy data [8, 20, 43, 46]. For instance, our own novel classifier, which is based on Temporal Convolution Networks (TCN) [5], can infer video streams even from short bursts of noisy measurements over the Internet (see §2 for details). Alternatively, a sensitive application could try to improve side-channel resilience by splitting traffic over multiple network paths [16, 54] or by using dedicated physical links that are not controlled by the adversary. However, such solutions are inadequate against a powerful adversary that can monitor a large fraction of the Internet [7] and may incur prohibitive network administration costs for small users on the Internet.

In contrast, a principled and practical approach to mitigating network side-channel leaks is *traffic shaping*. It involves modifying the victim's packet sizes and timing to make the resultant shape independent of secrets, so that an adversary cannot infer the secrets despite observing the (shaped) traffic.

Constant shaping involves sending fixed-sized packets at a constant rate, which is secure but incurs non-trivial bandwidth and/or latency overhead for applications with variable or bursty workloads [42]. Variable shaping strategies attempt to adapt traffic shapes to reduce the overhead at the cost of some privacy. However, the state-of-the-art (SOTA) variable shaping strategies rely on ad hoc heuristics that yield weak privacy guarantees [38, 55, 56] or unbounded privacy leaks [10, 11, 19, 24, 32]. Some techniques provide strong guarantees but require extensive a priori profiling of an applications' traffic to compute shapes [34, 63].

In addition to a shaping strategy, network side-channel mitigation also requires a robust implementation of packet padding and transmit scheduling. Many solutions attempt to protect traffic by controlling shaping from only one end of a communication (i.e., either a client or a server) and provide only best-effort protection [14, 33, 47]. Other solutions rely on trusting third-party mediators (e.g., Tor bridges), which implement shaping between the clients and mediators and between

the servers and mediators [36,59]. In Pacer [34], both application endpoints integrate a shaping system to comprehensively mitigate network side channels. However, Pacer encumbers application end hosts with non-trivial changes in the network stack to implement shaping, thus deterring adoption.

In this work, we address two main questions. First, is there an adaptive traffic shaping strategy that provides quantifiable and tunable privacy guarantees at runtime without requiring extensive pre-profiling of application traffic? Second, can traffic shaping be provided as a generic, portable, and efficient solution that can be integrated in different network settings and can support diverse applications?

We present NetShaper, a network side-channel mitigation system that answers both questions in the affirmative. First, NetShaper relies on a differential privacy (DP) based traffic shaping strategy, which provides quantifiable and tunable privacy guarantees. NetShaper specifies DP parameters for a configurable window of transmission. Moreover, it can configure the parameters independently for each direction of traffic on a communication link. The DP guarantees can be composed based on these parameters to achieve bounded privacy leaks for arbitrary bidirectional traffic. Overall, applications can tune the shaping based only on the privacy guarantees they desire and the overheads they can afford, and without the need for profiling their traffic. While strong privacy guarantees require DP parameters that incur large overheads, in practice, NetShaper can defeat SOTA attacks with even small amounts of DP noise, thus incurring low overheads.

Secondly, we present a traffic shaping tunnel with a modular endpoint design that can conceptually be integrated with any network stack and within any node. The tunnel implements padding and transmit scheduling of packets while adhering to the DP guarantees *by design*. By placing the tunnel endpoint in a middlebox at the edge of the private network, NetShaper can simultaneously protect the traffic of multiple applications. Moreover, the middlebox can amortize the shaping overheads among multiple flows without compromising the privacy for individual flows.

Together, the DP shaping strategy and NetShaper's tunnel provide effective network side-channel mitigation for diverse applications, such as video streaming and web services, with modest overheads. To the best of our knowledge, NetShaper is the first system to provide dynamic traffic shaping with quantifiable and tunable privacy guarantees based on DP.

**Contributions.** (i) We design a new attack classifier based on a Temporal Convolution Network (TCN) [5] and demonstrate its ability to infer videos streams from traffic shapes under noisy network traffic measurements in the Internet (§2). (ii) We model network side-channel mitigations as a differential privacy problem and provide a traffic shaping strategy that offers ($\varepsilon$,$\delta$)-differential privacy guarantees (§3). (iii) We design a QUIC-based traffic shaping tunnel and present a middlebox-based implementation of the tunnel, which supports traffic shaping while adhering to DP guarantees (§4). (iv) We demonstrate NetShaper's efficacy in defeating a SOTA classifier [43] and our new TCN classifier. We empirically evaluate the tradeoffs between NetShaper's privacy guarantees and performance overheads while mitigating network side-channel leaks in two classes of applications that have already been used in prior work, namely video streaming and web service (§5). (vi) We present a formal proof of NetShaper's differential privacy guarantees (§B).

## 2 Motivation and Overview

### 2.1 Network Side-Channel Attacks

Consider MedFlix, a fictitious medical video service that offers videos on symptoms, treatment procedures, and post-operative care. We demonstrate an example network side-channel attack. The goal is to infer from the traffic shape the videos being streamed by users. ISPs can aggregate such information to build per-user profiles and subsequently monetize them. Additionally, competitors might exploit network side channels to acquire corporate intelligence without detection.

We set up the video service and a video client as two Amazon AWS VMs placed in Oregon and Montreal, respectively. The video server hosts a dataset of 100 YouTube videos at 720p resolution with MPEG-DASH encoding [57]. The client streams the first 5 min of each video over HTTPS and collects the resulting network packet traces using tcpdump. We stream each video 100 times, thus collecting a total of 10,000 traces.

We reproduce Beauty and the Burst (BB) [43], a SOTA CNN classifier. We also present a new TCN classifier [5], which is robust to noisy measurements over the Internet. The classifiers' goal is to predict the video from a network trace. (We describe the classifiers in §A.) For each classifier, we transform each packet trace into a sequence of burst sizes transmitted within 1s windows and normalize the sequence by dividing each burst size by the total size of all bursts. We evaluate the performance of both classifiers with two datasets: a small dataset consisting of 40 videos with 4000 traces and a large dataset comprising all 100 videos (10000 traces). We train the classifiers for 1000 epochs with an 80-20 train-test split. BB's classification accuracy, recall, and precision with the small dataset are 0.61, 0.63, and 0.49, respectively, but all drop to 0.01 with the large dataset. TCN's accuracy, recall, and precision are all above 0.99 for both datasets.

Similarly, advanced ML classifiers are capable of identifying web traffic [8,46]. In general, classifiers will continue to evolve, increasing the adversary's capabilities to make inferences from noisy measurements. Hence, we need principled mitigations that address current SOTA attacks and achieve quantifiable leakage, which can be configured based on privacy requirements and overhead tolerance.

## 2.2 Key Ideas

A secure and practical network side-channel mitigation system must satisfy the following design goals: **G1.** Mitigate leaks through all aspects of the shape of transmitted traffic, **G2.** Provide quantifiable and tunable privacy guarantees for the communication parties, **G3.** Minimize overheads incurred while guaranteeing privacy, **G4.** Support a broad class of applications, and **G5.** Require minimal changes to applications.

NetShaper's shaping prevents leaks of the traffic content through sizes and timing of packets transmitted along each direction between application nodes (G1). In addition, NetShaper relies on the following three key ideas.

**Differentially private shaping.** Unlike constant shaping and variable-but-static shaping, dynamic shaping offers the most flexibility for adapting traffic shape at runtime based on workload patterns and, therefore, can significantly reduce overheads. Unfortunately, existing dynamic shaping techniques either have unbounded privacy leaks or offer only weak privacy guarantees. NetShaper's novel differential privacy (DP) based shaping strategy provides quantifiable and tunable bounds on privacy leaks, without relying on profiling of application traffic (G2). The DP guarantees are enforced on streams at the granularity of a sliding window of configurable length. Streams longer than this window length retain (weaker) DP guarantees through composition.

**Shaping in a middlebox.** NetShaper uses a tunnel abstraction to implement traffic shaping. The tunnel shapes application traffic such that an adversary observing the tunnel traffic cannot infer application secrets. In principle, a tunnel endpoint could be integrated with the application host (e.g., in a VM isolated from the end-host application) or in a separate node through which the application's traffic passes. NetShaper relies on the second approach and implements the tunnel endpoint as a middlebox, which could be integrated with an existing network element, such as a router, a VPN gateway, or a firewall. The middlebox implementation enables securing multiple applications without requiring modifications on individual end hosts (G4). Furthermore, it allows pooling multiple flows with the same privacy requirements in the same tunnel, which helps to amortize the per-flow overhead (G3).

**Minimal modifications to end applications.** By default, NetShaper shapes all traffic through a tunnel with a fixed differential privacy guarantee. However, an application can explicitly specify different DP parameters to adapt the privacy guarantee enforced for its traffic, as well as bandwidth and latency constraints and any prioritization preferences on a per-flow basis. This requires only a small modification in the application; it must transmit a shaping configuration message to the middlebox. Thus, NetShaper offers a balance between being fully application-agnostic and optimizing for privacy or overhead with minimal support from applications (G2, G5).

## 2.3 Threat Model

NetShaper's goal is to hide the content of an application's network traffic. We assume that the application endpoints are inside separate trusted private networks (e.g., each node is behind a VPN gateway node). We assume that the applications are non-malicious and do not leak the secrets themselves.

The adversary controls network links in the public Internet (e.g., ISPs) and can record, measure, and tamper with the victim's traffic as it traverses the links under the adversary's control. The adversary can precisely record the traffic shape—the sizes, timing, and direction of packets—between the gateway nodes. In particular, it may have access to observations of arbitrary known streams to train its attack. Furthermore, the adversary can drop, replay, or inject packets into the victim's traffic. However, it cannot infiltrate the private network, or the clients and servers within the private network (thus, no covert attacks). We do not consider threats due to observing the IP addresses of packets, although NetShaper can hide IP addresses of application end hosts behind a shared traffic shaping tunnel. We also do not consider the threat where a victim accidentally installs a malicious script in the browser, thus enabling an adversary to colocate with the victim's application and observe its traffic [34, 43]. This is a reasonable assumption, since a colocated adversary can exploit many other direct or indirect channels for data leaks that will be far more efficient than network side channels [22, 27, 31, 53, 61].

NetShaper does not address leaks of one application's sensitive data through the traffic shape of colocated benign applications transmitting only non-sensitive traffic. Such leaks can arise, for instance, due to microarchitectural interference among the applications colocated on a host or among their flows if they pass through shared links. NetShaper assumes that privacy-sensitive and privacy-insensitive applications are physically isolated and their flows use separate network paths. For instance, an application could be partitioned into separate instances, each dedicated to serving clients with similar privacy requirements (similar to performance-driven sharding). In practice, the end hosts could instead implement side-channel mitigations against colocated applications [9, 26, 34, 39, 45, 51] and combine NetShaper's traffic shaping with TDMA scheduling on network links [6, 52].

We present a middlebox-based NetShaper implementation that can be placed in front of an organization's gateway router. NetShaper's trusted computing base (TCB) includes all components in the organization's private network and the middleboxes. We do not address leaks of secrets due to bugs, vulnerabilities or side channels in the middleboxes. In practice, these could be mitigated using orthogonal techniques, such as software fault isolation [49], resource partitioning [30], and constant-time implementation techniques [4, 15, 62].

Under these assumptions, NetShaper prevents leaks of application secrets through the sizes and timing of packets transmitted in either direction between the application endpoints.

## 3 Differentially Private Traffic Shaping

The goal of differentially private shaping is to dynamically adjust packet sizes and timing based on the available data stream, while ensuring that the DP guarantees hold for any information that an adversary (§2.3) can observe. The adversary can observe sizes, inter-packet intervals, and directions of packets in sequences of arbitrary lengths. Given these observations, the specific DP guarantee that NetShaper provides is that the adversary cannot identify (i) the traffic content (e.g., video streams, web pages), and (ii) the presence of any one flow between two application endpoints. We start with a brief primer on DP and its key properties (§3.1). We then formalize the information available to an adversary observing an application's traffic and describe our building blocks for a differentially private shaping mechanism in §3.2. We describe our mechanism for sending data based on DP measurements in §3.3 and prove our guarantees in §3.4.

### 3.1 A Primer on Differential Privacy

Developed originally for databases, DP is a technique to provide aggregate results on a database without revealing information about individual database records. Formally, a randomized algorithm $\mathcal{M}$ is $(\varepsilon,\delta)$-DP if, for all $\mathcal{S} \subseteq \text{Range}(\mathcal{M})$ and for all databases $d, d'$ that differ in only one element, we have:

$$P[\mathcal{M}(d) \in \mathcal{S}] \leq e^{\varepsilon} P[\mathcal{M}(d') \in \mathcal{S}] + \delta \quad (1)$$

The parameter $\varepsilon$ represents the *privacy loss* of algorithm $\mathcal{M}$, i.e., given a result of $\mathcal{M}$, the information gain for any adversary on learning whether the input database is $d$ or $d'$ is at most $e^{\varepsilon}$ [25]. The $\delta$ is the probability with which $\mathcal{M}$ fails to bound the privacy loss to $e^{\varepsilon}$.

The difference between $d$ and $d'$ is called the *distance* between the databases. Traditionally, this distance is defined as the number of records that differ between $d$ and $d'$, and the DP guarantee is over any neighboring databases (at distance one). However, the DP definition extends to other distance metrics for use in specific settings [12, 29]. In NetShaper we also use a different distance, and hence neighboring, definition to define DP guarantees over dynamic traffic streams (§3.2).

Our shaping mechanism relies on three fundamental properties of DP. First, DP is resilient to post-processing: given the result $r$ of any $(\varepsilon,\delta)$-DP mechanism $\mathcal{M}$, any function $f(r)$ of the result is also $(\varepsilon,\delta)$-DP. As a result, any computation or decision made on a DP result is still DP with the same guarantees. Second, DP is closed under adaptive sequential *composition*: the combined result of two DP mechanisms $\mathcal{M}_1$ and $\mathcal{M}_2$ is also DP, though with higher losses ($\varepsilon$ and $\delta$). We use the Rényi-DP definition [35] to achieve simple but strong composition results and subsequently convert the results back to the standard DP definition. Third, DP is robust to auxiliary information: the guarantee from Equation 1 holds regardless of any side information known to an attacker. That is, an attacker knowing or controlling part of the database cannot extract more knowledge from a DP result than without this side information.

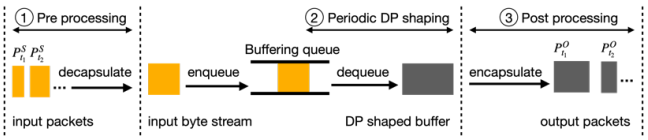


Figure 1: Overview of DP shaping

### 3.2 The Building Blocks

Figure 1 illustrates NetShaper's $(\varepsilon,\delta)$-DP shaping strategy. An application's input stream is a packet sequence $S = \{P_1^S, P_2^S, P_3^S, \ldots\}$, where $P_i^S = (l_i^S, t_i^S)$ indicates that the $i^{\text{th}}$ input packet in $S$ has length $l_i$ bytes and is transmitted at timestamp $t_i$. Without shaping, an adversary can precisely observe $S$ and infer the content, which is correlated with the stream [43].

Our DP shaping relies on two key ideas. First, it models the DP guarantees for the (potentially long) traffic streams in windows of fixed length $W$, denoted by $(\varepsilon_W,\delta_W)$-DP. An input sequence over window $j$ is a finite subsequence $S_j \subset S$, such that $S_j = \{P_i^S \mid P_i^S \in S \text{ and } t_i \in j\}$. NetShaper's DP guarantees cover all (overlapping) windows up to size $W$.

A key assumption for NetShaper's DP guarantees to hold over $W$-sized windows is that the tunnel can always transmit all incoming data from application streams within any $W$-sized time window. In other words, we assume:

**Assumption 1.** *All bytes enqueued prior to or at time $t$ are transmitted by time $t+W$.*

We explain how to realize this assumption in a tunnel design in §4. Under this assumption, the privacy loss of the complete traffic stream is simply a DP composition of the privacy losses over consecutive windows.

The window length $W$ is a configuration parameter, which is set before the start of an application's transmission. In practice, $W$ would be in the order of a few seconds.

Secondly, we use the primitive of a *buffering queue* to control the maximum information accessible by an adversary within each window. We denote the number of bytes present in the queue (i.e., length of the queue) by $L$. Conceptually, NetShaper extracts bytes from the input stream, $S$, and enqueues them. Further, we discretize time into $W$-sized windows and, at the beginning of each time window, NetShaper adds a DP noise to the queue length to determine the amount of data from the queue that should be transmitted as shaped traffic.

The shaped traffic is then transmitted as a packet sequence denoted by $O = \{P_1^O, P_2^O, P_3^O \dots\}$, which is observable by an adversary. While shaping requires discretizing transmit windows, the DP guarantees apply over arbitrary windows.

In the rest of this section, we focus on NetShaper's DP guarantees over a single window. We first formally define a notion of $(\varepsilon_W, \delta_W)$-DP privacy, which guarantees DP over transmission windows of length $W$. The guarantee applies over all $W$ windows, and applying DP composition yields guarantees over multiple windows. Then, we provide an overview of the DP shaping mechanism, which further samples noise in multiple shorter uniform intervals within each window. Finally, we prove how the shaping mechanism provides $(\varepsilon_W, \delta_W)$-DP.

To formalize NetShaper's DP guarantees, we first define a meaningful distance between any pair of streams in windows of length $W$ and the associated neighboring definition:

**Definition 1.** *Two streams $S_j$ and $S'_j$ transmitted in a window $j$ are neighbors if their L1-norm distance is at most $\Delta_W$ bytes in a window of upto length $W$, i.e., $\| S_j - S'_j \|_1 \leq \Delta_W$.*

$\Delta_W$ is the max L1-norm distance between each pair of application streams transmitted in any window $j$. We utilize the L1-norm (the sum of absolute values) as our distance metric to quantify the dissimilarity between two traffic streams, as it captures differences in both packet sizes and temporal pattern.

## 3.3 The Shaping Mechanism

**From windows to intervals.** Based on Assumption 1 and Definition 1, the window length $W$ affects the maximum number of bytes that can be accumulated in the buffering queue (thus, the maximum distance between stream pairs), as well as the transmission delay for the payload bytes enqueued. Specifically, large windows lead to high-latency bursty traffic. To reduce latency and burstiness, NetShaper further splits windows into smaller intervals of length $T$ and samples noise at the beginning of each interval. In absence of shaping, the queue length corresponds to the amount of unshaped traffic transmitted in an interval of $T$. The privacy loss over a window is now defined by applying DP composition on the privacy loss of individual intervals.

To apply noise in each interval, we now define the sensitivity of the queue length over intervals of length $T$. Sensitivity, denoted $\Delta_T$, is the maximum difference in the queue length over any interval $T$ that can be caused by changing one application stream to another. Formally, consider two alternative streams $S_j$ and $S'_j$ passing through the queue. Suppose that when transmitting $S_j$ (similarly $S'_j$), the queue length at the beginning of its $k^{\text{th}}$ interval is denoted by $L_k$ (respectively $L'_k$). Then:

$$\Delta_T = \max_{k=0}^{\lceil \frac{W}{T} \rceil} \max_{S_j, S'_j} |L_k - L'_k| \tag{2}$$

**Shaping overview.** NetShaper's DP shaping involves three steps as shown in Figure 1. (1) As application packets arrive in a window $w$, the preprocessing step extracts the payload bytes and enqueues them into the buffering queue. (2) In a periodic interval $k$, the core DP shaping algorithm performs a DP measurement, which entails sampling noise $z$ from a DP distribution and computing a DP burst size $\tilde{L}_k \triangleq L_k + z$. The shaping logic then prepares a *shaped buffer* of length $\tilde{L}_k$ with the application bytes available in the queue and dummy bytes if required. The DP shaping logic uses an additive Gaussian noise mechanism. The noise $z$ is sampled from a normal distribution $\mathcal{N}(\mu, \sigma^2)$ parameterized by $\varepsilon_T$, $\delta_T$, and $\Delta_T$: The mean $\mu$ is 0 and the variance $\sigma^2$ is given by $\frac{2\Delta_T^2}{\varepsilon_T^2} \ln(\frac{1.25}{\delta_T})$. If the sampled noise is negative, we retain some of the data in the queue until the next DP measurement interval. Given this noise distribution, one measurement is $(\varepsilon_T, \delta_T)$-DP. (3) Data in the shaped buffer is then split into one or more packets and transmitted to the network. Since these packets are a post-processing of the DP-shaped buffer, they preserve DP as long as no new dependency on private data is introduced. This last constraint requires the packets' size and transmit time to be selected independently of the data. We describe how NetShaper enforces this constraint in §4.2.

The privacy loss ($\varepsilon_W$) and bandwidth overheads of the DP shaping (represented by $\sigma_T$, i.e., the standard deviation of the noise distribution function) depend on $W$, $\Delta_W$, and the number of intervals $N = \lceil \frac{W}{T} \rceil$ in $W$. Additionally, the latency overheads depend on $T$. Note that for a specific value of $\Delta_W$ and $N$, the DP guarantee $\varepsilon_W$ is fully specified by $\sigma_T$, and remains the same even at different time scales. That is, scaling $W$ and $T$ proportionally does not change the privacy and overhead costs. We analyze the impact of different choices for these parameters on the privacy guarantees and overheads in §5. Here, we focus on a formal model of the DP guarantees.

## 3.4 Privacy Guarantees

At a high level, analyzing the $(\varepsilon_W, \delta_W)$-DP guarantee of the overall shaping mechanism requires two steps: (i) showing that the difference in the buffering queue length is bounded for neighboring streams for all transmissions of the streams (Prop. 1), and (ii) composing the DP cost of each measurement over the intervals defining a window of length $W$ (Prop. 2).

We first show that the sensitivity of each measurement $\Delta_T$ is at most the window sensitivity $\Delta_W$:

**Proposition 1.** *NetShaper enforces $\Delta_T \leq \Delta_W$.*

*Proof sketch.* Consider any two streams $S_j$ and $S'_j$, as in Equation 2. The proof proceeds in two steps. First, under Assumption 1, streams can accumulate queued traffic for at most $W$, so two different streams can create a difference $|L_k - L'_k|$ of at most $\Delta_W$. Second, dequeuing can only make two different queues closer: Consider measurement time $k$, with queue

lengths $L_k > L'_k$ (the opposite case is symmetric). For a DP noise draw $z$, we have $\tilde{L}_k > \tilde{L}'_k$. Since shaping sends at least as much data under $\tilde{L}_k$ as under $\tilde{L}'_k$, but no more than $\tilde{L}_k - \tilde{L}'_k$, after dequeuing we have $|L'_{k+1} - L_{k+1}| \leq |L'_k - L_k|$. In summary, the maximum queue difference under two different streams $\Delta_T$ can grow to at most $\Delta_W$ due to data queuing, and dequeuing only decreases that difference, and hence $\Delta_T \leq \Delta_W$. The complete proof is in §B. □

We can then reason about DP guarantees over intervals of length $T$ in order to achieve the privacy loss for the entire window of length $W$. Formally, we have:

**Proposition 2.** *NetShaper enforces* $(\varepsilon_W, \delta_W)$*-DP, with* $\varepsilon_W, \delta_W \triangleq DP\_compose(\varepsilon_T, \delta_T, \lceil \frac{W}{T} \rceil)$.

*Proof.* By Prop. 1, the sensitivity of each measurement is at most $\Delta_W$. By the Gaussian DP mechanism, the measured queue size $\tilde{L}_k$ in each interval $k$ of length $T$ is $(\varepsilon_T, \delta_T)$-DP. Using DP composition over $\lceil \frac{W}{T} \rceil$ $(\varepsilon_T, \delta_T)$-DP measurements, and the fact that $O$ is a post-processing of DP measurements, yields the $(\varepsilon_W, \delta_W)$-DP over any $W$ length window. □

We use Rényi-DP composition on the Gaussian mechanism for DP_compose(). Note that the overhead (i.e., noise added) due to DP does not depend on the number of streams: the overhead is the same regardless of the number of streams transmitted through the buffering queue simultaneously.

**Summary.** By buffering all data in a queue, and periodically deciding the size of the data to send over the network with a DP measurement, NetShaper's shaping algorithm makes the shape of traffic (volume of data sent over time) DP with regards to the application's original traffic sequence. Thus, as long as no observable characteristics of the traffic directly depend on application secrets (the original traffic sequence), the observable outbound traffic is DP.

## 4 Traffic Shaping Tunnel

The previous section describes an abstract differentially private traffic shaping strategy. We now present NetShaper's traffic-shaping tunnel.

A tunnel must address three requirements. First, it must satisfy DP guarantees. For this, the tunnel must complete DP measurements and prepare shaped packets within each interval, and it must be able to transmit all payload bytes generated from an application within a finite window length (as defined in the DP strategy). Secondly, the payload and dummy bytes in the shaped packets must be indistinguishable to an adversary. For this, the payload and dummy bytes must be transmitted through a shared transport layer so that they are identically acknowledged by the receiver and subject to congestion control and loss recovery mechanisms. Finally, the tunnel must provide similar levels of reliability, congestion control, and loss recovery as expected by the application.

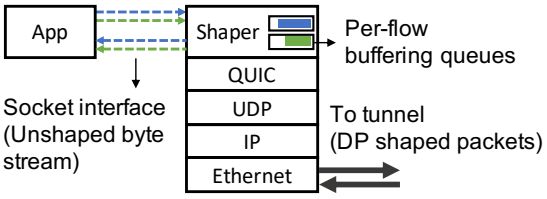


Figure 2: Overview of tunnel design (one endpoint)

Figure 2 shows the design of one endpoint of NetShaper's traffic shaping tunnel. A similar endpoint is deployed on the other end of the tunnel. The shape of the traffic in the tunnel can be configured independently in each direction. The privacy loss in bidirectional streams is the DP composition of the privacy loss in each direction.

A tunnel endpoint consists of a shaping layer (Shaper) on top of QUIC, which in turn runs on top of a standard UDP stack[1]. The tunnel endpoints establish a bidirectional QUIC connection and generate DP-sized transmit buffers in fixed intervals, which carry payload bytes from one or more application flows. In the absence of application payload, a tunnel endpoint transmits dummy bytes, which are discarded at the other endpoint. QUIC encrypts all outbound packets.

NetShaper adopts a transport-layer proxy architecture: each application terminates a connection with its local tunnel endpoint. The application byte stream is sent to the remote application over three piecewise connections: (i) between the application and its local tunnel endpoint, (ii) between the tunnel endpoints, and (iii) between the remote tunnel endpoint and the remote application. This ensures only one active congestion control and reliable delivery mechanism in the tunnel and that all bytes are subject to identical mechanisms[2].

The application and the tunnel endpoint shown in Figure 2 could either be colocated on the same host or located on separate hosts. For example, the tunnel endpoint could be on a separate middlebox or integrated with a gateway at the edge of an organization's network. In each case, the traffic between the application and the tunnel endpoint is assumed to be unobservable to an adversary. Our design (§4.1) does not distinguish between the two configurations. Our implementation (§4.2) assumes that the tunnel endpoint is located on a separate middlebox.

### 4.1 Tunnel Design and Operations

**Tunnel setup and teardown.** Before applications can communicate with each other, a NetShaper tunnel must be set up

[1] Instead of QUIC/UDP, NetShaper could also use a traditional TCP stack.

[2] We discard tunneling TCP through TCP as it causes TCP meltdown [2, 21], or TCP through UDP as it is unsafe. (TCP between the application hosts would retransmit lost payload bytes only, not any dummy bytes injected between the tunnel endpoints, making the dummy bytes observable.)

between their local tunnel endpoints. The initiator application sends a configuration message to its local tunnel endpoint with the source and destination IP addresses and ports, a reliability flag, and a privacy descriptor. The reliability flag indicates if the tunnel should provide reliable delivery semantics or not. The privacy descriptor indicates the DP parameters to be used for shaping the tunnel traffic.

Upon receiving a configuration message, the Shaper establishes a QUIC connection with the remote tunnel endpoint and configures the reliability semantics and privacy parameters for each direction. It also initializes three types of bidirectional streams in the tunnel: control, dummy, and data streams. One *control stream* is used to transmit messages related to the establishment and termination of a connection between the application endpoints. A *dummy stream* transmits padding in QUIC packets in the form of STREAM frames[3]. The tunnel pre-configures a finite number of data streams, which carry payload bytes from one or more application flows.

When the tunnel is inactive for a period of time, one of the tunnel endpoints initiates a termination sequence and closes all open QUIC streams and the tunnel connection.

**Connection establishment and termination.** Once a tunnel is ready, applications can establish and terminate connections with each other, which is mediated by the tunnel. When the initiator application runs a connection establishment handshake with its local tunnel endpoint, the Shaper maps the application flow to a per-flow buffering queue and one of the inactive QUIC data streams in the tunnel, and notifies the remote tunnel endpoint. The remote tunnel endpoint establishes a connection with the receiver application and maps the receiver application's flow with the data stream. The connection termination handshake is handled similarly by the tunnel endpoints. The messages for connection establishment and termination are transmitted over the control stream in the tunnel and shaped according to the tunnel's parameters.

**Outbound traffic shaping.** The Shaper accumulates the outbound bytes of an application flow in a buffering queue before it transmits them in packets whose sizes and timing follow a distribution that guarantees DP. Within a tunnel, the Shaper transmits bytes from all active flows into a differentially-private packet sequence. At periodic intervals, called DP measurement intervals, it performs a DP measurement on the per-flow queues to determine the number of bytes $\tilde{L}$ to be transmitted according to the tunnel's DP parameters. It prepares a *shaped buffer* consisting of $R$ payload bytes and $D$ dummy bytes, where $R$ is the minimum of $\tilde{L}$ and the application bytes available in the buffering queues, and $D = \tilde{L} - R$, which may lie between 0 and $\tilde{L}$. The Shaper then passes the buffer with the position and length of the padding to QUIC.

[3]We do not use QUIC's PADDING frames as they do not elicit acknowledgements and hence are distinguishable from STREAM frames [23].

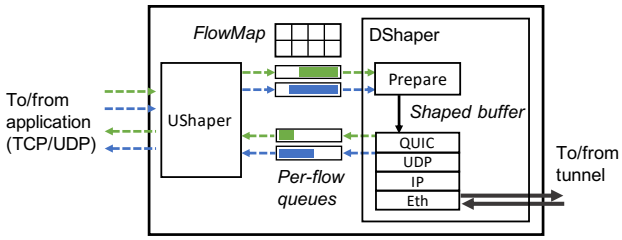


Figure 3: NetShaper middlebox design

QUIC transforms the shaped buffer into one or more STREAM frames based on the congestion window, the flow window of the receiver endpoint, and the MTU (maximum transmission unit). It places the padding bytes into a dummy STREAM frame. QUIC packages the frames into packets, whose length is at most MTU minus the length of the headers and whose payload is encrypted. QUIC forwards the packets to the UDP layer, which subsequently transmits the prepared packets as quickly as it can, given the line rate of the NIC.

NetShaper configures the DP measurement interval such that the Shaper can prepare each shaped buffer within an interval. If the preparation time for a buffer exceeds the interval, the Shaper discards the buffer. This ensures that the buffering queue length does not grow significantly, which in turn controls the overhead incurred due to DP shaping. We evaluate the impact of the length of the buffering queue and the DP measurement interval on privacy guarantees, bandwidth overheads, and latency overheads in §5.

**Inbound traffic processing.** A tunnel endpoint receives shaped packets from the tunnel and applies inverse processing on each packet. QUIC receives the packet and sends an ACK to the sender. Subsequently, it decrypts the packet, discards the dummy frame, and forwards the payload bytes from the remaining STREAM frames to the application.

## 4.2 Middlebox Implementation

We present a middlebox-based NetShaper implementation. Recall from §2.2, a middlebox can support shaping for several applications and amortizes the shaping cost among multiple flows that share the same tunnel. Moreover, middleboxes can support "long-term" tunnels between endpoints. Such tunnels may be set up, for instance, between organization campuses to secure all communication between the campuses without the need for modifying individual application hosts.

For ease of implementation, our prototype requires applications to explicitly connect to the middleboxes. In principle, NetShaper can transparently proxy application connections.

In our implementation, a middlebox consists of two userspace processes. The `UShaper` mediates *unshaped* traffic between the applications and the middleboxes. The `DShaper` handles *DP shaped* traffic within the tunnel.

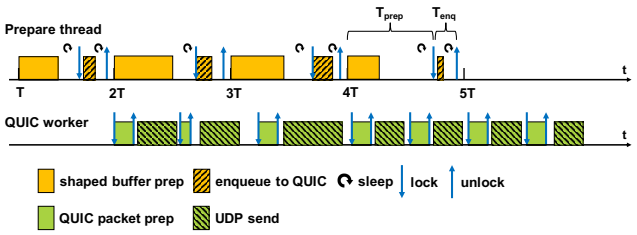


Figure 4: `DShaper` schedule

**UShaper.** The `UShaper` implements a transport server (or client) for interfacing with each local client (or server, respectively) application[4]. For managing multiple flows, it shares a `FlowMap` table with the `DShaper`, which consists of an entry for each end-to-end flow. Each entry maps the piecewise connections with a pair of transmit and receive queues to carry the local application's byte stream, and shaping configurations (e.g., privacy descriptor) provided by an application at the time of flow registration.

The `UShaper` receives the outbound traffic from a sender application and enqueues the byte stream into a per-flow transmit queue shared with the `DShaper`. It also dequeues bytes from a per-flow receive queue, repackages them into transport packets and sends them to the receiver application.

**DShaper.** The `DShaper` consists of a `Prepare` thread and a QUIC worker thread. The `Prepare` thread instantiates a QUIC client/server to establish a tunnel with the remote middlebox and implements the DP shaping logic. On the transmit side, `Prepare` prepares shaped buffers based on DP measurements of the transmit queues and then submits shaped buffers to the QUIC worker for transmission. On the receive size, the QUIC worker transmits ACK frames to the sender and then decrypts the QUIC packets, extracts the STREAM frames, and copies bytes (including dummy bytes) from each frame into the appropriate per-flow receive queue.

**Ensuring secret-independent shaping.** To enforce DP guarantees, `DShaper` could *transmit* exactly $\tilde{L}$ bytes in each DP measurement interval $T$. This would require ensuring: **P1.** `Prepare` computes $\tilde{L}$, allocates and prepares a buffer of length $\tilde{L}$, and passes the buffer to the QUIC worker within $T$, **P2.** the QUIC worker prepares encrypted packets from the buffer and sends them to UDP, such that the total payload size of the QUIC packets prepared in $T$ is $\tilde{L}$, and **P3.** the UDP stack transmits packets totaling to $\tilde{L}$ payload bytes to the NIC in $T$. Enforcing all these properties would produce a strict time-triggered schedule for each component, which would significantly reduce link utilization and increase packet latencies.

[4]The `UShaper` could also be a SOCKS5 proxy [1].

Thanks to DP post processing, however, it suffices to ensure the property P1, and **P4.** that the QUIC worker transforms the shaped buffer into network packets independently of the application data No other constraint on the sizes and timing of network packets is required to preserve DP.

Satisfying P1 involves one challenge. Although the application is physically isolated from the middlebox, its flow control behavior could be secret-dependent and could affect the middlebox's execution. For instance, the presence or absence of payload traffic from an application can affect the time `DShaper` requires to prepare the shaped buffers.

Thus, `DShaper` satisfies P1 as follows. (See Figure 4 for reference.) First, `Prepare` guarantees that a DP measurement $\tilde{L}$ is performed every fixed time interval $T$. Secondly, `Prepare` guarantees that a shaped buffer of length $\tilde{L}$ is *prepared* within a fixed time $T_{prep}$ within each interval $T$. Thirdly, `Prepare` locks the shaped buffer for a fixed time, $T_{enq}$, during which it enqueues the buffer for a QUIC worker. This ensures that the buffer is completely enqueued before QUIC starts transmitting it and that QUIC receives the buffer only at fixed delays.

We empirically profile the time taken by `Prepare` for preparing and enqueueing shaped buffers for various DP lengths. We set $T_{prep}$ and $T_{enq}$ to maximum values determined from profiling, and $T$ to the sum of these maximum values, i.e., $T_{max}$. If `Prepare` takes time less than $T_{prep}$ (or $T_{enq}$, respectively) to prepare (or enqueue) a shaped buffer, it sleeps until the end of the interval before moving to the next phase.

To satisfy P4, `Prepare` and QUIC worker threads run on separate cores sharing only the shaped buffers. `UShaper` runs on yet a different core and shares the `FlowMap` and the per-flow transmit queues containing unshaped traffic only with `Prepare`. It shares the per-flow receive queues with the QUIC worker, but they contain only shaped frames from the QUIC worker. Thus, the execution of the QUIC worker becomes independent of DP measurements in `Prepare`.

Variations in `Prepare`'s execution due to the state of the per-flow queues are masked by $T_{max}$, while QUIC's execution depends only on shaped buffers and thus, is secret-independent. Consequently, the packetization of shaped buffers in the QUIC worker and the UDP stack is secret-independent and any variations in packet transmit times induced due to their execution constitute post-processing noise.

## 4.3 Security Analysis

NetShaper provides the following security property: an adversary cannot infer application secrets from observing tunnel traffic. This property is ensured by a combination of a secure shaping strategy, the tunnel design, and implementation.

**S1. Secure shaping strategy.** The tunnel transmits traffic in differentially private-sized bursts in fixed intervals. Thus, the overall shape is DP. The proof of DP is in §B.

**S2. Secure tunnel design.** (i) The privacy guarantees of a tunnel are configured before the start of application transmis-

sion and do not change during the tunnel's lifetime. (ii) The tunnel mediates control between the end hosts, e.g., by transmitting custom connection establishment and termination messages. These messages are subject to the same DP shaping as the payload traffic (§4.1). (iii) The payload and dummy bytes in network packets are indistinguishable because all payload and dummy bytes are packaged into QUIC packets and encrypted uniformly. Moreover, QUIC handles acknowledgements, congestion control, and loss recovery for both payload and dummy bytes uniformly (§4.1).

**S3. Secure middlebox implementation.** (i) The unshaped traffic between an end host and its local middlebox is not visible to an adversary. (ii) `DShaper` follows the tunnel design in transmitting payload and dummy bytes. (iii) The sizes and timing of transmitted packets are secret-independent, because the time required for `Prepare` to prepare and enqueue shaped buffers is masked to secret-independent times. The subsequent packetization of buffers in QUIC is secret-independent (§4.2) and thus retains DP guarantees after post-processing. Any delays in transmitting the buffers can arise only due to congestion or packet losses in the tunnel network, which are secret-independent events.

## 5 Evaluation

Our evaluation answers the following questions. (i) How well does NetShaper mitigate state-of-the-art network side-channel attacks? (ii) What are the overheads associated with varying DP relevant configuration parameters? (iii) What are the packet latency overheads and the peak line rate and throughput sustained by our NetShaper middlebox? (iv) What are NetShaper's overall costs on privacy, bandwidth, client latency, and server throughput for different classes of applications? (v) How do NetShaper's privacy guarantees and performance overheads compare to prior techniques?

For our experiments, we use four AMD Ryzen 7 7700X desktops each with eight 4.5 GHz CPUs, 32 GB RAM, 1 TB storage, and one Marvell AQC113CS-B1-C 10Gbps NIC. We simulate client and server applications on two of the desktops and NetShaper's middleboxes on the other two desktops. The middleboxes are connected to each other via an additional Intel X550-T2 10Gbps NIC on each desktop. The client and server desktops are connected to one of the two middleboxes each via the Marvell NICs, overall forming a linear topology.

We implemented the `UShaper` and `DShaper` processes in 1100 and 1800 lines of C++ code, respectively, and deployed them on Ubuntu OS 22.04.02 (kernel version 5.19). NetShaper relies on the MSQUIC implementation of QUIC, libmsquic v2.1.8, which includes OpenSSL for traffic encryption, contributing an additional 180713 LoC to NetShaper's TCB.

For rapid evaluation, we built a simulator, which implements the `Prepare` thread's DP logic. The simulator transforms an application's original packet sequence (from tcpdump) into a sequence of burst sizes within fixed-length intervals, and outputs a sequence of transmit sizes corresponding to DP measurements. We confirmed that the bandwidth overheads from the simulator closely match the overheads observed on the testbed. Thus, we report privacy and bandwidth overhead results from the simulator and latency and throughput results from the testbed, unless specified otherwise.

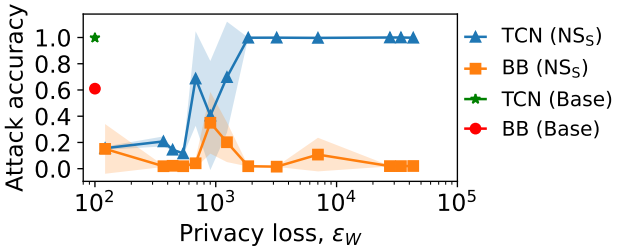


Figure 5: Classifier accuracy on shaped traces.

For all experiments, we use one baseline setup and one of three NetShaper configurations. In the baseline setup (**Base**), the client is directly connected to the server. In the simulator setup ($\mathbf{NS_S}$), we generated sequences of shaped burst sizes using DP shaping. With NetShaper, the traffic between the client and the server passes through two middleboxes, each implementing `UShaper` and `DShaper`. We consider two configurations of the middleboxes: (i) $\mathbf{NS_M}$: `DShaper` does not implement shaping (i.e., neither DP noise sampling nor the fixed length loop interval $T_{max}$), allowing us to measure the system overheads due to the middlebox implementation, and (ii) **NS**: `DShaper` implements the full shaping mechanism. By default, each middlebox is configured with 128 pairs of per-flow transmit and receive queues (unless specified otherwise). We configure the queue sizes for the max data that can be transmitted at line rate for a given DP measurement interval.

We use two applications for case studies, a video streaming service and a medical web service, which we describe below.

**Video service.** The video streaming service is hosted on an Nginx 1.23.4 web server and is used to serve 100 YouTube videos in 720p resolution. The videos are stored on a standard file system on the host OS and have durations ranging from 5 min to 130.3 min (median 12.6 min) and sizes ranging from 2.7 MB to 1.4 GB (median 73.7 MB). We implement a custom video streaming client in Python, which requests individual 5s segments synchronously from the service. The client uses one TCP connection for a single video stream.

**Web service.** The web service is also hosted on Nginx 1.23.4 and is used to serve a corpus of 100 static HTML pages of a medical website. The web pages are stored on a standard file system on the host OS and have sizes ranging from 54 KB to 147 KB (median: 90 KB). As a client, we use a modified wrk2 [3] that issues concurrent asynchronous HTTPS GET requests at a specified rate.

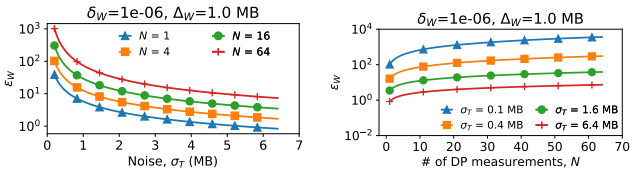


(a) (b)

Figure 6: Per-window privacy loss ($\varepsilon_W$) as a function of (a) noise ($\sigma_T$), and (b) number of DP measurements ($N$).

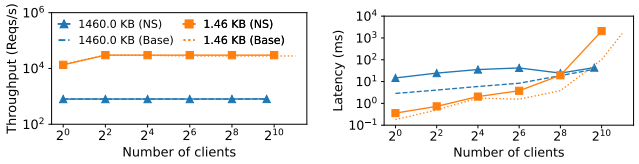


(a) # clients vs throughput (b) # clients vs latency

Figure 7: Throughput and latency overhead due to middleboxes without shaping.

## 5.1 NetShaper Defeats Attack Classifiers

We start with an empirical evaluation of the privacy offered by NetShaper's traffic shaping. Recall that the traffic shaping depends on several DP parameters: the window length $W$, the sensitivity for neighboring streams $\Delta_W$, the length of the DP measurement interval $T$, and the privacy loss $\varepsilon_W$. We evaluated the classifiers from §2.1 on shaped traffic generated using various values of these DP relevant parameters. We present the classifiers' performance based on only one set of values for $W$, $\Delta_W$, and $T$, while varying $\varepsilon_W$ between [100, 43000]. Our goal is to provide intuition about what values of $\varepsilon_W$ are sufficient to thwart a side-channel attack.

We set (i) $W = 5s$ to align with the 5s video segments that comprise the videos, (ii) $\Delta_W = 1MB$, which covers 97% of the video streams in our dataset (§C), and (iii) $T = 1s$, which leads to composing the privacy loss over $N = 5$ DP measurements of the buffering queues. The interval of 1s provides a reasonable trade-off between the privacy loss due to multiple DP measurements, the bandwidth overhead, and the latency overhead incurred while shaping individual video segments, which we discuss in the subsequent sections.

We used 40 videos of 5 min duration each. We streamed each video 100 times through our testbed without shaping and collected the resulting tcpdump traces. For each value of $\varepsilon_W$, we transformed each unshaped trace into a shaped trace using our simulator to generate a total of 4000 shaped traces. We transform the shaped traces and train the classifiers as in §2.1.

Figure 5 shows the average (markers) and the standard deviation (shaded region) of the accuracy of each classifier over three runs on the shaped traces. While BB does not perform well for nearly all values of $\varepsilon_W$, TCN can be thwarted only for $\varepsilon_W < 1000$. The BB and TCN accuracy on unshaped traffic (**Base**) is 0.61 and 0.99, respectively (§2.1). In conclusion, *while $\varepsilon_W \approx 100$ is too large to offer meaningful theoretical privacy guarantees, it is sufficient to defeat SOTA attacks.*

## 5.2 Impact of Privacy Parameters

We now evaluate how $\varepsilon_W$ varies with $\sigma_T$, $N$, and $\Delta_W$. Due to space constraints, we present plots for a fixed value of $\Delta_W = 1MB$ and defer additional plots for different values of $\Delta_W$ to §C. We analyze the impact of $W$ and $T$ on latency overheads separately. All analyses use $\delta_W = 10^{-6}$.

Figure 6a shows the trade-off between privacy loss ($\varepsilon_W$) and noise ($\sigma_T$) over four different numbers of DP measurements ($N$). Intuitively, a larger $\sigma_T$ implies higher bandwidth overhead due to DP shaping. To retain a total privacy loss $\varepsilon_W = 1$ with at most 4 DP measurements, we need to add noise with $\sigma_T = 6MB$ for each DP measurement. In contrast, $\varepsilon_W = 100$ with 4 DP measurements (approx. configuration that defeats the classifiers in §5.1) only requires $\sigma_T < 0.1MB$. We discuss how to amortize bandwidth overheads using concurrent flows without increasing privacy loss in §5.4 and §5.5.

Figure 6b shows that the total privacy loss escalates with an increase in the number of DP measurements. While fewer measurements within a window (thus larger decision intervals) help to lower the total privacy loss, the trade-off is the higher latency overhead, which we discuss in §5.4 and §5.5.

Using these plots, an application can choose suitable values of $\Delta_W$ and $W$ to determine the trade-off between $\varepsilon_W$ and $\delta_W$. For our web application serving static HTML, we recommend $W = 1s$, since web page downloads in our AWS setup (§2.1) finished within 1s, and $\Delta_W = 150KB$, which covers 95% of the web pages in our dataset. §5.1 explained the choices for our video application. Using $\varepsilon_W$ and $T$, we can further determine the aggregate privacy loss over longer traffic streams using Rényi-DP composition. For instance, with $\varepsilon_W = 1$, $W = 5s$, and $T = 1s$, the total privacy loss for a 5 min video, which generates 300 DP measurements at 1s intervals, is 8.92; the total loss for a 1 hr video is 38.8. We emphasize that $\Delta_W$ *and* $\varepsilon_W$ *should be selected using trade-off plots similar to Figure 6 and independently of the application's dataset.*

## 5.3 Performance Microbenchmarks

We now turn our attention to experiments to determine the overheads on per-packet latencies and the peak line rate and throughput sustainable by a NetShaper middlebox.

**Middlebox throughput.** We measure the peak throughput (requests/s) attained by a server application, the response latency experienced by the clients, and the impact on this throughput and latency due to the middleboxes. We restrict Nginx to one worker thread and one core on the server desktop. We evaluate using two object sizes: 1.4 KB (one MTU)

and 1.4 MB. We identify the peak request rate that can be handled by a single wrk2 client, then increase the clients until we find the peak throughput the server can provide. We then vary the number of concurrent clients while generating the peak request load sustainable by the server to find the maximum number of concurrent clients that the server can handle and to measure the impact on the response latency.

We run experiments for 3 min and discard the measurements from the first minute to eliminate startup effects. Figure 7a shows the average of the peak throughput observed across 3 runs. The standard deviation is below 1% in all cases. For 1.4 KB and 1.4 MB objects, the **Base** server achieves a peak throughput of 30K req/s (64 clients) and 800 req/s (800 clients), respectively. $\mathbf{NS_M}$ matches the peak throughput and the max concurrent clients sustained by **Base**.

**Latency.** Figure 7b shows the average and standard deviation of the response latencies over a 2 min run. The ping latency between each pair of directly connected desktops is $0.56 \pm 0.18$ ms. This overhead comes from the fact that each packet traverses four additional network stacks (across two middleboxes) in each direction. This also involves data copy operations between the kernel and user space. The data copy overhead is proportional to the object size; thus $\mathbf{NS_M}$'s latency overhead increases with the larger response sizes. The kernel overhead including data copy overheads are not fundamental to NetShaper's design.

By using kernel bypass techniques or tools like DPDK [18], NetShaper can eliminate data copies between user and kernel space and reduce the latency overhead.

**Shaping interval, preparation, and enqueue times.** We further profile the middlebox execution to measure the max latencies of the two components in the `Prepare` loop (§4.2): the preparation of the shaped buffer and queuing of the buffer to QUIC worker. These measures determine the maximum durations for preparing and enqueueing shaped buffers ($T_{prep}$ and $T_{enq}$, respectively), and the minimum value for the shaping interval $T$. We profile the delays with the middlebox configured with 128 queues. This implies that our middlebox can support a maximum of 128 concurrent clients. One can profile the delays for a different number of queues to support a different number of concurrent clients.

Based on our measurements, we set $T_{prep} = 6ms$ and $T_{enq} = 1ms$. The smallest value for $T$ that we can configure is 10ms.

**Throughput and latency with shaping enabled.** We now re-run the microbenchmarks with **NS** configuration. We use three different configurations for $T$: 10ms, 50ms, and 100ms. We use 128 concurrent clients. The middlebox can sustain the peak throughput of 30K req/s with 1.4KB objects and 700 req/s with 1.4MB objects for each configuration of $T$. For 1.4KB objects, the average and standard deviation of the response latency with the three configurations are as follows: (i) $T = 10ms$: $30.47 \pm 3.89$ ms, (ii) $T = 50ms$: $51.39 \pm 14.64$ ms, (iii) $T = 100ms$: $77.49 \pm 28.96$ ms. For 1.4MB objects, the latencies are as follows: (i) $T = 10ms$: $41.31 \pm 10.84$ ms, (ii) $T = 50ms$: $76.96 \pm 21.12$ ms, (iii) $T = 100ms$: $127.48 \pm 45.69$ ms. The latency is dominated by the $T$ configuration. The high variance in the latency is due to shaping. If a request arrives just after the decision loop has prepared a buffer in the current iteration, the request will be delayed by at least one iteration of the loop. Moreover, a negative sampling of DP noise may lead to a smaller DP measurement than the available payload bytes in the buffering queues, thus delaying the requests by one or more intervals. This effect is particularly enhanced in a workload close to the line rate. Thus, NetShaper can perform well within about 12-15% of the line rate.

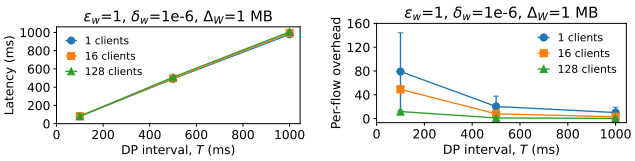


(a) Latency vs DP interval (b) BW overhead vs DP interval

Figure 8: Video streaming. Latency and bandwidth overhead for different values of DP interval.

**CPU utilization.** The CPU utilization is 3-10% for the `Prepare` core and depends on the DP measurement interval; the utilization is 8-70% for the QUIC worker core, which depends on the network I/O. The `UShaper` core utilizes 100% of the CPU as it polls for packets from `Prepare`. As such, the `Prepare` and QUIC worker cores would be able to support additional tunnel instances by time-sharing their core. By using a polling interval, we could reduce the CPU utilization of `UShaper` to support additional requests at the cost of additional latency. In general, multiple tunnels can time-share the same physical cores, as long as each core runs the same type of thread, to suffice property P4 mentioned in Section 4.2.

## 5.4 Case Study: Video Streaming

Next, we examine the effect of different privacy settings on bandwidth and latency overheads for video streaming clients.

We run experiments with three values of the DP measurement interval $T$ for the server: 100ms, 500ms, and 1s, and we use $\Delta_W = 1MB$ and $\varepsilon_W = 1$. For all experiments, we set the DP parameters for client request traffic as follows: $\Delta_W = 200$ bytes, $W = 1s$, $T = 10ms$, and $\varepsilon_W = 1$. We run experiments with 1, 16, and 128 video clients; each client requests one video randomly selected from the dataset. For each set of configurations, we measure the average response latency for individual video segments with the testbed as well

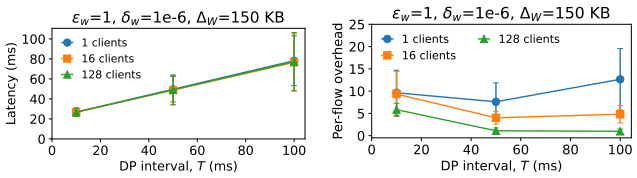


(a) Latency vs DP interval (b) BW overhead vs DP interval

Figure 9: Web service. Latency and bandwidth overhead for different values of DP interval.

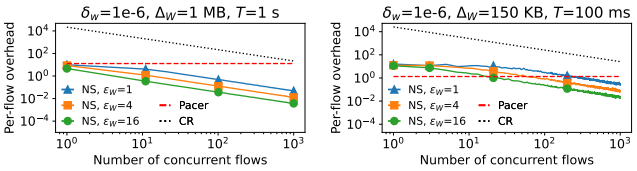


(a) Video streaming. (b) Web service.

Figure 10: Relative bandwidth overheads of NetShaper (**NS**), constant shaping (**CR**), and Pacer.

as the per-flow relative bandwidth overhead for the video streams in the simulator.

**Latency and bandwidth overhead.** Figures 8a and 8b respectively show the average segment download latency and the average per-flow relative bandwidth overhead as a function of different intervals and for varying number of clients. The **Base** segment download latency is 2.86 $\pm$ 1.41ms. The latency variance is due to variances in the segment sizes. The relative bandwidth overhead of a video is the number of dummy bytes transmitted normalized to the size of the unshaped video stream. The error bars show the standard deviation in latency and bandwidth overhead.

First, Figure 8a shows that, for all values of $T$, the video segments can be downloaded well within 5s, which is the time to play each segment and request the next segment from the server. Secondly, the results show the trade-off between latency and bandwidth. A larger DP measurement interval implies higher download latency but fewer measurements and lower noise added to the payload, thus yielding a lower bandwidth overhead. Thirdly, with multiple concurrent streaming clients, the bandwidth overhead is amortized, while the average download latency only depends on $T$. Overall, NetShaper's shaping can secure video streams with low bandwidth overheads and no impact on the streaming experience.

## 5.5 Case Study: Web Service

We perform similar experiments as §5.4 with our web service. For the server responses, we use $\Delta_W = 150KB$, $W = 1s$, and $\varepsilon_W = 1$. For $T$, we use 10ms, 50ms, and 100ms. For the client requests, we use the same configs as in §5.4. We run 3 min experiments with 1, 16, and 128 wrk2 clients with a total load of 1600 req/s for both configurations; each client requests random web pages from the dataset. We discard the numbers of the first minute.

**Latency and bandwidth overhead.** Figures 9a and 9b respectively show the average response latency and the average per-web page relative bandwidth overhead, across all web page requests. The **Base** latency is 0.225 $\pm$ 0.3 ms. (The high variance is due to the time precision in wrk2 being restricted to 1ms.) The web workload is more sporadic than video streaming, thus web page download latencies have higher variance than video segment download latency. The absolute latency overhead for **NS** depends on the choice of $T$. The relative overhead depends on the underlying network latency, which unlike our testbed, is in the order of 10s to 100s of milliseconds in the Internet. Interestingly, the bandwidth overhead for web traffic first reduces with increasing DP measurement interval from 10ms to 50ms, but then increases again with an interval of 100ms. This is because, for small web pages, the DP interval of 100ms is larger than the total time required to download web pages. As a result, additional overhead is incurred due to the padding of traffic in the 100ms intervals.

## 5.6 Comparison with other techniques

Figures 10a and 10b show the per-flow relative bandwidth overhead of **NS** for video and web applications, respectively, for varying with number of concurrent flows and for different values of $\varepsilon_W$. We also compare with the overheads that would be incurred due to constant rate shaping (**CR**) and Pacer [34], a SOTA system that provides dynamic shaping on a per-client request basis.

For **CR**, we configure the peak load for video service corresponding to transmitting 1.7MB in every 5s, and the peak load for web service corresponding to transmitting 57KB every 50ms. These rates correspond to transmitting at a rate that covers the largest object sizes in our video and web datasets.

In Pacer, for video service, we pad a segment at $i^{\text{th}}$ index in a video stream to the largest segment size at that index across all videos in the dataset. For web service, we pad all web pages to the largest page size, i.e., 147KB in our dataset.

For both video and web traffic, **NS** incurs three orders of magnitude lower overhead than **CR**, which requires continuously transmitting traffic at the peak server load (configured for 1000 clients).

For video traffic, while **NS** incurs similar overhead as Pacer for a single flow with $\varepsilon_W = 1$, it can further amortize its overheads among multiple concurrent streams within the tunnel without compromising privacy. For web traffic, **NS** requires more than 20 flows to achieve lower overhead than Pacer. Pacer shapes server traffic only upon receiving a client request and does not shape client traffic. Thus, it leaks the timing and

shape of client requests, which could potentially reveal information about the server responses [13]. NetShaper shapes traffic in both directions, which incurs higher overhead at the cost of stronger privacy than Pacer.

**Evaluation summary.** Our evaluation provides four insights. (i) There is a huge gap between the theoretical DP guarantees and the privacy configurations required to defeat SOTA attacks. (ii) The latency overhead is dominated by the choice of DP measurement interval, (iii) NetShaper's middlebox can match about 88% of the 10Gbps NIC line rate; a single core of `UShaper` can match the peak throughput of a single core server, (iv) NetShaper's cost is in the two additional cores for `Prepare` and QUIC worker, which helps to avoid any secret-dependent interference in shaping and keep low DP measurement loop lengths. By optimising the implementation, we could use a single middlebox to support larger workloads.

## 6 Related Work

We discuss prior work along three axes: shaping strategy, system architecture, and threat model and goals.

**Traffic shaping for web.** Prior work has used traffic shaping strategies for defending against website fingerprinting attacks. These strategies can be classified into two types: static and dynamic. Walkie-Talkie [56], Supersequence [55], and Glove [38] use clustering techniques to group objects of a corpus and then shape the traffic of all objects within each cluster to conform to a similar pattern. Traffic morphing [60] makes the traffic of one page look like that of another. These techniques compute traffic shapes that envelope or resemble the network traces of individual objects. Therefore, they require a large number of traces to account for variations in traffic shapes due to dynamic network conditions. In contrast, NetShaper is computationally less expensive because it dynamically adapts traffic shapes based on the prevailing network conditions.

Cs-BuFLO [10], Tamaraw [11], and DynaFlow [32] are dynamic techniques that determine traffic shape at runtime. Tamaraw, Cs-BuFLO, and DynaFlow pad object sizes to values that are correlated with the original object sizes, such as the next multiple or power of a configurable constant. The constants determine the padding overhead. These defenses provide privacy akin to k-anonymity, which Tamaraw formalizes [11]. NetShaper provides a strong privacy guarantee based on DP (see §D for a proof).

**Traffic shaping for videos.** Zhang et al. [63] generate differentially private shapes for video streams using the Fourier Perturbation Algorithm (FPA) [41]. FPA transforms an input trace, which is a finite time series of bursts, into a series of DP shaped bursts of the same length. Consequently, FPA cannot guarantee transmission of the entire input byte stream within the shaped trace. Unlike FPA, NetShaper dynamically determines DP burst lengths for each transmit interval.

**Pacer.** NetShaper's shaping tunnel is similar to Pacer's [34] cloaked tunnel. However, they have different threat models. Pacer [34] mitigates leaks of a Cloud tenant's secrets to a colocated adversary through contention at shared network links. Pacer controls the transmit time of TCP packets in accordance with the shaping schedule and congestion control signals. Thus, Pacer's tunnel endpoint requires non-trivial changes to the network stack on the end hosts. NetShaper focuses on applications behind private networks that communicate using the public Internet. Hence, we can place NetShaper's tunnel endpoints at the interface of the private-public networks, thus supporting multiple applications without modifying end hosts. Moreover, by shaping above the transport layer, NetShaper needs to control only the precise timing for generation of bursts of DP length and not the subsequent packetization and transmission to the network.

**Censorship circumvention proxies.** Tor [48], FTE [17], Scramblesuit [59], Skypemorph [36] are censorship circumvention systems that rely on traffic obfuscation, scrambling, and transformations of a sensitive application's shape to that of a non-sensitive application. These techniques prevent identification of original protocols by deep packet inspection. But, unlike NetShaper, they do not prevent inference of secrets from traffic shapes.

**Metadata private communication.** Karaoke [28] and Vuvuzela [50] use constant traffic shaping among participants, but use differential privacy to hide participants in a message conversation. NetShaper is different because it provides differentially private traffic shaping to hide the traffic content. In principle, it is possible to combine NetShaper's DP traffic shaping within a DP message-passing system to provide both content privacy and anonymity.

## 7 Conclusion

NetShaper is a provably secure network side-channel mitigation system that provides quantifiable and tunable privacy guarantees in traffic shaping. We believe that NetShaper can eliminate the arms race in network side-channel attacks and defenses and can provide a portable and configurable framework for deploying mitigations for applications with diverse traffic characteristics and in different settings. NetShaper's differential privacy based traffic shaping strategy as well as its modular and portable tunnel design can be extended to mitigate leaks in multi-node systems, but we leave the details to future work.

## References


[1] Pluggable Transports. https://obfuscation.github.io/. Last accessed on 6 Jun 2023.

[2] What is TCP Meltdown? https://openvpn.net/faq/what-is-tcp-meltdown/. Accessed on Apr 30, 2023.

[3] wrk2: A constant throughput, correct latency recording variant of wrk. https://github.com/giltene/wrk2.

[4] José Bacelar Almeida, Manuel Barbosa, Gilles Barthe, François Dupressoir, and Michael Emmi. Verifying Constant-Time Implementations. In *USENIX Security Symposium*, 2016.

[5] Shaojie Bai, J Zico Kolter, and Vladlen Koltun. An Empirical Evaluation of Generic Convolutional and Recurrent Networks for Sequence Modeling. *arXiv:1803.01271*, 2018.

[6] Andrew Beams, Sampath Kannan, and Sebastian Angel. Packet scheduling with optional client privacy. In *ACM Conf. on Computer and Communications Security (CCS)*, 2021.

[7] Matthias Beckerle, Jonathan Magnusson, and Tobias Pulls. Splitting Hairs and Network Traces: Improved Attacks Against Traffic Splitting as a Website Fingerprinting Defense. In *Workshop on Privacy in the Electronic Society (WPES)*, 2022.

[8] Sanjit Bhat, David Lu, Albert Kwon, and Srinivas Devadas. Var-cnn: A data-efficient website fingerprinting attack based on deep learning. In *Privacy Enhancing Technologies Symposium (PETS)*, 2019.

[9] Benjamin A Braun, Suman Jana, and Dan Boneh. Robust and efficient elimination of cache and timing side channels. *arXiv preprint arXiv:1506.00189*, 2015.

[10] Xiang Cai, Rishab Nithyanand, and Rob Johnson. CS-BuFLO: A Congestion Sensitive Website Fingerprinting Defense. In *Workshop on Privacy in the Electronic Society (WPES)*, 2014.

[11] Xiang Cai, Rishab Nithyanand, Tao Wang, Rob Johnson, and Ian Goldberg. A systematic approach to developing and evaluating website fingerprinting defenses. In *ACM SIGSAC Conference on Computer and Communications Security (CCS)*, 2014.

[12] Konstantinos Chatzikokolakis, Miguel E Andrés, Nicolás Emilio Bordenabe, and Catuscia Palamidessi. Broadening the Scope of Differential Privacy Using Metrics. In *Privacy Enhancing Technologies Symposium (PETS)*, 2013.

[13] Shuo Chen, Rui Wang, XiaoFeng Wang, and Kehuan Zhang. Side-Channel Leaks in Web Applications: A Reality Today, a Challenge Tomorrow. In *IEEE Symposium on Security and Privacy (SP)*, 2010.

[14] Giovanni Cherubin, Jamie Hayes, and Marc Juarez. Website Fingerprinting Defenses at the Application Layer. In *Privacy Enhancing Technologies Symposium (PETS)*, 2017.

[15] Bart Coppens, Ingrid Verbauwhede, Koen De Bosschere, and Bjorn De Sutter. Practical Mitigations for Timing-Based Side-Channel Attacks on Modern x86 Processors. In *IEEE Symposium on Security and Privacy (S&P)*, 2009.

[16] Wladimir De la Cadena, Asya Mitseva, Jens Hiller, Jan Pennekamp, Sebastian Reuter, Julian Filter, Thomas Engel, Klaus Wehrle, and Andriy Panchenko. TrafficSliver: Fighting Website Fingerprinting Attacks with Traffic Splitting. In *ACM SIGSAC Conference on Computer and Communications Security (CCS)*, 2020.

[17] Kevin P Dyer, Scott E Coull, Thomas Ristenpart, and Thomas Shrimpton. Protocol misidentification made easy with format-transforming encryption. In *ACM Conf. on Computer and Communications Security (CCS)*, 2013.

[18] Linux Foundation. Data plane development kit (DPDK), 2015.

[19] Jiajun Gong and Tao Wang. Zero-delay Lightweight Defenses against Website Fingerprinting. In *USENIX Security Symposium*, 2020.

[20] Jamie Hayes and George Danezis. k-fingerprinting: A Robust Scalable Website Fingerprinting Technique. In *USENIX Security Symposium*, 2016.

[21] Osamu Honda, Hiroyuki Ohsaki, Makoto Imase, Mika Ishizuka, and Junichi Murayama. Understanding TCP over TCP: effects of TCP tunneling on end-to-end throughput and latency. In *Performance, Quality of Service, and Control of Next-Generation Communication and Sensor Networks III*, volume 6011, pages 138–146, 2005.

[22] Gorka Irazoqui, Thomas Eisenbarth, and Berk Sunar. S$A: A Shared Cache Attack That Works across Cores and Defies VM Sandboxing–and Its Application to AES. In *IEEE Symposium on Security and Privacy (SP)*, 2015.

[23] Jana Iyengar and Martin Thomson. QUIC: A UDP-Based Multiplexed and Secure Transport. RFC 9000, May 2021.

[24] Marc Juarez, Mohsen Imani, Mike Perry, Claudia Diaz, and Matthew Wright. Toward an Efficient Website Fingerprinting Defense. In *European Symposium on Research in Computer Security (ESORICS)*, 2016.

[25] Shiva P Kasiviswanathan and Adam Smith. On the 'semantics' of differential privacy: A bayesian formulation. *Journal of Privacy and Confidentiality*, 2014.

[26] Taesoo Kim, Marcus Peinado, and Gloria Mainar-Ruiz. STEALTHMEM: System-Level Protection Against Cache-Based Side Channel Attacks in the Cloud. In *USENIX Security Symposium*, 2012.

[27] Paul Kocher, Jann Horn, Anders Fogh, , Daniel Genkin, Daniel Gruss, Werner Haas, Mike Hamburg, Moritz Lipp, Stefan Mangard, Thomas Prescher, Michael Schwarz, and Yuval Yarom. Spectre Attacks: Exploiting Speculative Execution. In *IEEE Symposium on Security and Privacy (S&P)*, 2019.

[28] David Lazar, Yossi Gilad, and Nickolai Zeldovich. Karaoke: Distributed private messaging immune to passive traffic analysis. In *USENIX Symposium on Operating Systems Design and Implementation (OSDI)*, 2018.

[29] Mathias Lecuyer, Vaggelis Atlidakis, Roxana Geambasu, Daniel Hsu, and Suman Jana. Certified robustness to adversarial examples with differential privacy. In *IEEE Symposium on Security and Privacy (SP)*, 2019.

[30] Fangfei Liu, Qian Ge, Yuval Yarom, Frank Mckeen, Carlos Rozas, Gernot Heiser, and Ruby B Lee. CATalyst: Defeating last-level cache side channel attacks in cloud computing. In *IEEE International Symposium on High Performance Computer Architecture (HPCA)*, 2016.

[31] Fangfei Liu, Yuval Yarom, Qian Ge, Gernot Heiser, and Ruby B Lee. Last-level cache side-channel attacks are practical. In *IEEE Symposium on Security and Privacy (SP)*, 2015.

[32] David Lu, Sanjit Bhat, Albert Kwon, and Srinivas Devadas. DynaFlow: An Efficient Website Fingerprinting Defense Based on Dynamically-Adjusting Flows. In *Workshop on Privacy in the Electronic Society (WPES)*, 2018.

[33] Xiapu Luo, Peng Zhou, Edmond WW Chan, Wenke Lee, Rocky KC Chang, and Roberto Perdisci. HTTPOS: Sealing Information Leaks with Browser-side Obfuscation of Encrypted Flows. In *Network and Distributed System Security Symposium (NDSS)*, volume 11, 2011.

[34] Aastha Mehta, Mohamed Alzayat, Roberta De Viti, Björn B Brandenburg, Peter Druschel, and Deepak Garg. Pacer: Comprehensive Network {Side-Channel} Mitigation in the Cloud. In *USENIX Security Symposium*, 2022.

[35] Ilya Mironov. Rényi differential privacy. In *2017 IEEE 30th computer security foundations symposium (CSF)*, pages 263–275. IEEE, 2017.

[36] Hooman Mohajeri Moghaddam, Baiyu Li, Mohammad Derakhshani, and Ian Goldberg. Skypemorph: Protocol Obfuscation for Tor Bridges. In *ACM Conf. on Computer and Communications Security (CCS)*, 2012.

[37] Milad Nasr, Alireza Bahramali, and Amir Houmansadr. Defeating DNN-Based Traffic Analysis Systems in Real-Time With Blind Adversarial Perturbations. In *USENIX Security Symposium*, 2021.

[38] Rishab Nithyanand, Xiang Cai, and Rob Johnson. Glove: A Bespoke Website Fingerprinting Defense. In *Workshop on Privacy in the Electronic Society (WPES)*, 2014.

[39] Dan Page. Partitioned cache architecture as a side-channel defence mechanism, 2005.

[40] Mohammad Saidur Rahman, Mohsen Imani, Nate Mathews, and Matthew Wright. Mockingbird: Defending Against Deep-Learning-Based Website Fingerprinting Attacks with Adversarial Traces. *IEEE Transactions on Information Forensics and Security*, 16:1594–1609, 2020.

[41] Vibhor Rastogi and Suman Nath. Differentially private aggregation of distributed time-series with transformation and encryption. In *Proceedings of the 2010 ACM SIGMOD International Conference on Management of data*, pages 735–746, 2010.

[42] T Scott Saponas, Jonathan Lester, Carl Hartung, Sameer Agarwal, Tadayoshi Kohno, et al. Devices That Tell on You: Privacy Trends in Consumer Ubiquitous Computing. In *USENIX Security Symposium*, 2007.

[43] Roei Schuster, Vitaly Shmatikov, and Eran Tromer. Beauty and the Burst: Remote Identification of Encrypted Video Streams. In *USENIX Security Symposium*, 2017.

[44] Shawn Shan, Arjun Nitin Bhagoji, Haitao Zheng, and Ben Y Zhao. Patch-based Defenses against Web Fingerprinting Attacks. In *ACM Workshop on Artificial Intelligence and Security (AISec)*, 2021.

[45] Jicheng Shi, Xiang Song, Haibo Chen, and Binyu Zang. Limiting cache-based side-channel in multi-tenant cloud using dynamic page coloring. In *IEEE/IFIP Intl. Conf. on Dependable Systems and Networks Workshops (DSN-W)*, 2011.

[46] Payap Sirinam, Mohsen Imani, Marc Juarez, and Matthew Wright. Deep fingerprinting: Undermining website fingerprinting defenses with deep learning. In

*ACM SIGSAC Conference on Computer and Communications Security (CCS)*, 2018.

[47] Jean-Pierre Smith, Luca Dolfi, Prateek Mittal, and Adrian Perrig. QCSD: A QUIC Client-Side Website-Fingerprinting Defence Framework. In *USENIX Security Symposium*, 2022.

[48] Paul Syverson, Roger Dingledine, and Nick Mathewson. Tor: The Second-Generation Onion Router. In *Usenix Security*, 2004.

[49] Gang Tan. Principles and Implementation Techniques of Software-Based Fault Isolation. *Foundations and Trends® in Privacy and Security*, 1(3):137–198, 2017.

[50] Jelle Van Den Hooff, David Lazar, Matei Zaharia, and Nickolai Zeldovich. Vuvuzela: Scalable private messaging resistant to traffic analysis. In *Symposium on Operating Systems Principles (SOSP)*, 2015.

[51] Venkatanathan Varadarajan, Thomas Ristenpart, and Michael M Swift. Scheduler-based Defenses against Cross-VM Side-channels. In *USENIX Security Symposium*, 2014.

[52] Bhanu Chandra Vattikonda, George Porter, Amin Vahdat, and Alex C Snoeren. Practical TDMA for Datacenter Ethernet. In *ACM European Conference on Computer Systems (EuroSys)*, 2012.

[53] Pepe Vila and Boris Köpf. Loophole: Timing Attacks on Shared Event Loops in Chrome. In *USENIX Security Symposium*, 2017.

[54] Mona Wang, Anunay Kulshrestha, Liang Wang, and Prateek Mittal. Leveraging strategic connection migration-powered traffic splitting for privacy. In *Privacy Enhancing Technologies*, 2022.

[55] Tao Wang, Xiang Cai, Rishab Nithyanand, Rob Johnson, and Ian Goldberg. Effective Attacks and Provable Defenses for Website Fingerprinting. In *USENIX Security Symposium*, 2014.

[56] Tao Wang and Ian Goldberg. Walkie-Talkie: An Efficient Defense Against Passive Website Fingerprinting Attacks. In *USENIX Security Symposium*, 2017.

[57] Cedric Westphal, Stefan Lederer, Christopher Mueller, Andrea Detti, Daniel Corujo, Jianping Wang, Marie-Jose Montpetit, Niall Murray, Christian Timmerer, Daniel Posch, Aytac Azgin, and Will Liu. RFC 7933: Adaptive Video Streaming over Information-Centric Networking (ICN). https://datatracker.ietf.org/doc/html/rfc3168. Accessed on Apr 30, 2023.

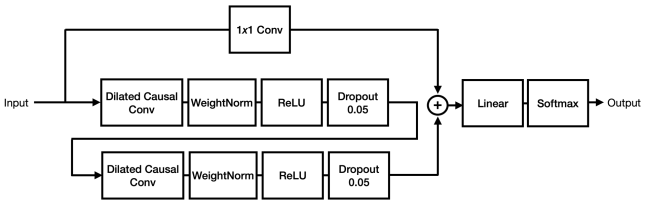


Figure 11: TCN classifier

[58] White, Andrew M and Matthews, Austin R and Snow, Kevin Z and Monrose, Fabian. Phonotactic reconstruction of encrypted voip conversations: Hookt on fon-iks. In *IEEE Symposium on Security and Privacy (S&P)*, 2011.

[59] Philipp Winter, Tobias Pulls, and Juergen Fuss. ScrambleSuit: A Polymorphic Network Protocol to Circumvent Censorship. In *ACM Workshop on Privacy in the Electronic Society (WPES)*, 2013.

[60] Charles V. Wright, Scott E. Coull, and Fabian Monrose. Traffic morphing: An efficient defense against statistical traffic analysis. In *Network and Distributed System Security Symposium (NDSS)*, 2009.

[61] Yuval Yarom and Katrina Falkner. FLUSH+RELOAD: A High Resolution, Low Noise, L3 Cache Side-Channel Attack. In *USENIX Security Symposium*, 2014.

[62] Danfeng Zhang, Aslan Askarov, and Andrew C Myers. Predictive Mitigation of Timing Channels in Interactive Systems. In *ACM Conf. on Computer and Communications Security (CCS)*, 2011.

[63] Xiaokuan Zhang, Jihun Hamm, Michael K Reiter, and Yinqian Zhang. Statistical Privacy for Streaming Traffic. In *ISOC Network and Distributed System Security Symposium (NDSS)*, 2019.

## A Attack classifiers

**Beauty and Burst.** The Beauty and the Burst classifier (BB) [43] is a CNN (convolutional neural network) consisting of three convolution layers, a max pooling layer, and two dense layers. We use a dropout of 0.5, 0.7, and 0.5 between the hidden layers of the network. We train the classifier with an Adam optimizer, a categorical cross-entropy function, a learning rate of 0.01, with a batch size of 64, and for 1000 epochs.

**Temporal Convolution Network** While CNNs are generally effective in sequence modelling, they look at future samples in a sequence and a very limited history of past samples to decide the output of the current sample. Consequently, they require a large number of traces and long traces for effective training and prediction.

Temporal Convolutional Networks (TCNs) [5] overcome these problems of CNNs by utilizing a one-dimensional fully-convolutional network equipped with causal dilated convolutions, which allow them to examine deep into the past to produce an output for the sequence at any given moment.

Figure 11 shows the architecture of our TCN classifier, which follows the architecture proposed by Bai et al. [5]. It consists of two dilated causal convolutional layers, followed by weight normalization and dropout layers with a dropout probability of 0.05. We train the classifier for 1000 epochs.

## B Proof of NetShaper's DP based Shaping

**Proposition.** *NetShaper enforces* $\Delta_T \leq \Delta_W$.

To prove the proposition stated above, we will first establish the following lemma.

**Lemma.** *Assume two neighboring traffic streams,* $S_j$ *and* $S'_j$ *(*$\|S_j - S'_j\|_1 \leq \Delta_W$*), transmitted through NetShaper. If both streams are reshaped to the same output stream, O, then by the end of any interval of shaping execution, the length of the buffering queue for the first and second streams are* $\Delta_W$*-close. In other words we have:*

$$\forall k \geq 0 : |L_k - L'_k| \leq \Delta_W \tag{3}$$

*Proof.* NetShaper dequeues data from the buffering queue periodically at intervals of $T$ seconds. Thus, while transmitting a stream $S$, the length of the buffering queue at the end of $k^{\text{th}}$ interval, $T_k$ is a function of three variables:

1. The length of the buffering queue at the end of $(k-1)^{\text{th}}$ interval, $L_{k-1}$.
2. The total number of payload bytes that have been dequeued from the buffering queue in the $k^{\text{th}}$ interval, $R_k$.
3. The number of new payload bytes from the application stream added to the buffering queue since the previous interval, which is the sum of sizes of all packets arriving between $(k-1)^{\text{th}}$ and $k^{\text{th}}$ interval, i.e., $\sum_{T_{k-1} \leq t < T_k} P_t^S$.

As two streams are reshaped to the output stream, $O$, the DP burst size for two streams is the same in all intervals (i.e. $\forall k \geq 0 : \tilde{L}_k = \tilde{L}'_k$).

Therefore, the length of the buffering queue after dequeue in the $k^{\text{th}}$ interval is given by:

$$L_k = L_{k-1} + \sum_{T_{k-1} \leq t < T_k} P_t^S - R_k \tag{4}$$

Based on Equation 4, the difference between queue lengths of two neighboring streams, $S_j, S'_j$ at $k^{th}$ interval is:

$$\begin{aligned} L_k - L'_k \;=\; & (L_{k-1} - L'_{k-1}) + \\ & \Big(\sum_{T_{k-1} \leq t < T_k} P_t^S - \sum_{Tk-1 \leq t < T_k} P_t^{S'}\Big) - (R_k - R'_k) \end{aligned} \tag{5}$$

We divide the proof into two different steps. First, we show that the dequeue stage of the shaping mechanism does not increase the difference in queue lengths. Secondly, we show that under Assumption 1, the enqueue stage of incoming streams does not increase the difference in queue lengths beyond $\Delta_W$.

Suppose $S_j$ and $S'_j$ are reshaped to the same output stream, $O$. Thus, the sizes of output packets generated in each decision interval $T$ when transmitting either streams is the same. However, the content of the output packets in each stream may differ based on the sizes and timing of the packets in each input stream. For the shaping mechanism, this implies that the number of payload bytes dequeued from the buffering queue for when transmitting each stream may not necessarily match. Nevertheless, the shaping mechanism always satisfies the following inequality:

$$(L_k - L'_k).(R_k - R'_k) \geq 0 \tag{6}$$

To show why Equation 6 always holds, we consider all the possible scenarios for two queue lengths after $k^{\text{th}}$ interval:

1. $L_k, L'_k > 0$: This indicates that there are still some untransmitted payload bytes remaining in the buffering queue for both streams. Consequently, it implies that the shaping mechanism does not add any dummy bytes to compensate for the difference between the DP burst size and the amount of data in the queues. We also know that the DP burst size for two streams are the same ($\tilde{L}_k = \tilde{L}'_k$) Therefore: $R_k = R'_k \rightarrow R_k - R'_k = 0$.
2. $L_k,\ L'_k = 0$: This simply implies $L_k - L'_k = 0$
3. $L_k = 0,\ L'_k > 0$: The DP burst size is the same for both queues. Thus, the first queue provided less payload data since it has emptied out. This means: $R_k \leq R'_k$.
4. $L'_k = 0,\ L_k > 0$: This is symmetric to the previous case.

Now, using Equation 6, we prove the following:

$$|L_k - L'_k| \leq |L_{k-1} - L'_{k-1}| + \sum_{T_{k-1} \leq t < T_k} |P_t^S - P_t^{S'}| \tag{7}$$

Let's consider $(L_k - L'_k) \geq 0$. (The case of $(L'_k - L_k) \geq 0$ is symmetric.) Using Equation (5), we get:

$$\begin{aligned} |L_k - L'_k| &= L_k - L'_k \\ &= (L_{k-1} - L'_{k-1}) + \Big(\sum_{T_{k-1} \leq t < T_k} P_t^S - P_t^{S'}\Big) - (R_k - R'_k) \\ &\leq (L_{k-1} - L'_{k-1}) + \Big(\sum_{T_{k-1} \leq t < T_k} P_t^S - P_t^{S'}\Big) \\ &\leq \Big|(L_{k-1} - L'_{k-1}) + \Big(\sum_{T_{k-1} \leq t < T_k} P_t^S - P_t^{S'}\Big)\Big| \\ &\leq |L_{k-1} - L'_{k-1}| + \sum_{T_{k-1} \leq t < T_k} |P_t^S - P_t^{S'}| \end{aligned}$$

Intuitively, this means the dequeue stage, never increases the difference between two queues lengths. Now, we show that under Assumption 1, the difference in queue lengths is bounded.

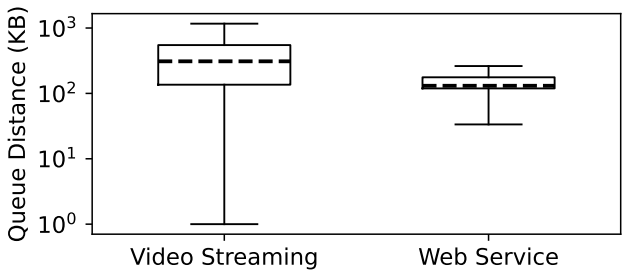


Figure 12: Distribution of the difference in buffering queue lengths for pairs of an application's streams.

With $d_k = |L_k - L'_k|$ and $d_0 = 0$, we have:

$$\begin{aligned} d_k &\leq d_{k-1} + \sum_{T_{k-1} \leq t < T_k} |P_t^S - P_t^{S'}| \\ &= 0 + \sum_{i=0}^{k} \Big( \sum_{T_{i-1} \leq t < T_i} |P_t^S - P_t^{S'}| \Big) \\ &= \sum_{0 \leq t < T_k} |P_t^S - P_t^{S'}| \\ &= \sum_{0 \leq t < T_k - W} |P_t^S - P_t^{S'}| + \sum_{T_k - W \leq t < T_k} |P_t^S - P_t^{S'}| \\ &= 0 + \|S_j - S'_j\|_1 \leq \Delta_W \end{aligned}$$

□

To conclude, the maximum difference between queue lengths (i.e., the sensitivity, $\Delta_T$) is always bounded by $\Delta_W$.

$$\Delta_T = \max_{k=0}^{\lceil \frac{W}{T} \rceil} \max_{S_j, S'_j} |L_k - L'_k| \leq \Delta_W \tag{8}$$

## C Extended evaluation of privacy loss vs noise overheads

Figure 13 shows the relation between per-window privacy loss ($\varepsilon_W$), noise overhead in MB ($\sigma_W$), sensitivity in MB ($\Delta_W$), and number of DP measurements ($N$) at a lower scale of sensitivity ($\Delta_W$) for two different setups: applications with high sensitivity values (e.g. 10 MB) where the queue size undergoes significant changes across different streams and applications with low sensitivity (e.g. 0.1 MB).

In addition, the boxplot in Figure 12 shows the distribution of the difference in buffering queue lengths generated for each pair of an application's streams. The shaping window length $W$ is assumed to be 5s for video streams and 1s for web pages. The error bars show the minimum and maximum differences, and the boxes show the first and third quartiles. The dashed lines show the median difference, which is 300 KB and 130 KB for video streaming and web service, respectively.

## D Comparison of NetShaper and Tamaraw

Prior work has proposed several shaping strategies, although many of them use ad hoc heuristics for shaping various features of network traffic to mitigate network side-channel leaks. Tamaraw [11] provides a mathematical notion of privacy guarantee of a shaping strategy, called $\varepsilon$-security. To disambiguate with NetShaper's notion of $(\varepsilon_W, \delta_W)$-DP, we rename Tamaraw's $\varepsilon$ variable with $\gamma$ in this section.

We show that NetShaper's $(\varepsilon_W, \delta_W)$-DP definition is strictly stronger than Tamaraw's $\gamma$-security definition.

We start by explaining Tamaraw's definition. Tamaraw defines $W$ as the random variable that represents the label of a traffic trace. For each traffic trace, $w$, let $T_w$ $T_w^D$ be the random variables representing the packet trace of $w$ before and after applying shaping on $w$ respectively. The distribution of $T_w^D$ encompasses all variations in observed patterns of a trace $w$ resulting from both the defense mechanism and the network, and the distribution of $T_w$ only captures the randomness added in the network. The attacker can measure the distribution of $W$ and $T_w^D$ independently.

Upon observing a trace $t$ on the network, an optimal attack $A$, selects the label that corresponds to the maximum likelihood of observing that trace.

$$A(t) = \operatorname*{argmax}_w \Pr[W = w] \Pr[T_w^D = t]$$

For any attack $A$, we represent the probability that attack output the label $w_i$ with $\Pr_A[w_i]$.

**Definition** (Tamaraw $\gamma$-privacy)**.** *A fingerprinting defense $D$ is said to be uniformly $\gamma$-private if for the attack $\mathcal{A}$ if we have:*

$$\max_w \left[ \Pr[A(T_w^D) = w] \right] \leq \gamma$$

**Proposition.** *Tamaraw $\gamma$-privacy is strictly weaker than the notion of $\varepsilon$-differential privacy.*

To prove the above proposition, we need to prove the following two lemmas.

**Lemma 1.** *There exists a Tamaraw $\gamma$-private defense mechanism that fails to satisfy $(\varepsilon)$-differential privacy for any given value of $\varepsilon$.*

*Proof.* Consider a web service with a dataset of $n$ web pages. We propose the following defense mechanism, $D$, with two parameters $\alpha$ and $\beta$:

1. For the webpage $w_i : i = j$, $D$ reshapes it to the constant-rate pattern, $O_c$, with probability $\beta$. Otherwise, with probability $1 - \beta$, it reveals the original traffic pattern of the webpage, $T_{w_{i=j}}$.

2. For any webpage $w_i : i \in \{1, 2, \ldots, j-1, j+1, \ldots, n\}$, $D$ reshapes it to the constant-rate pattern, $O_c$, with probability $\alpha$ such that $\alpha > e^{\varepsilon}\beta$. Otherwise, $D$ reveals the original pattern of $w_i$, $T_{w_{i \neq j}}$, with probability $\alpha$.

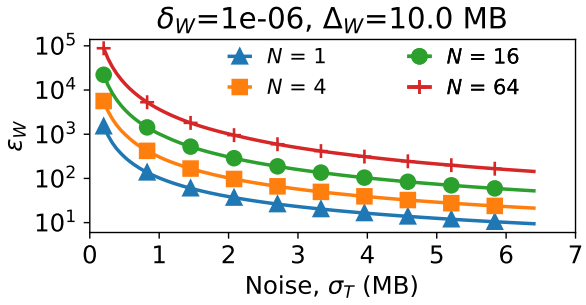


(a) Noise vs privacy loss

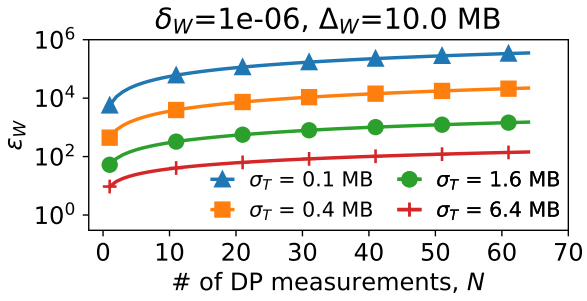


(b) Number of DP updates vs privacy loss

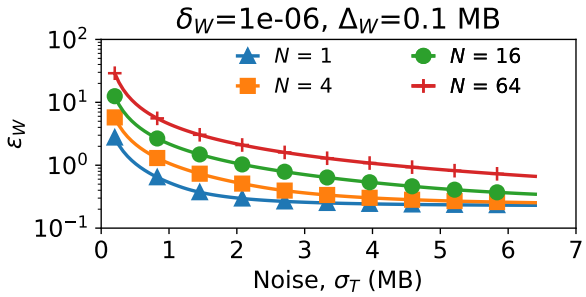


(c) Noise vs privacy loss

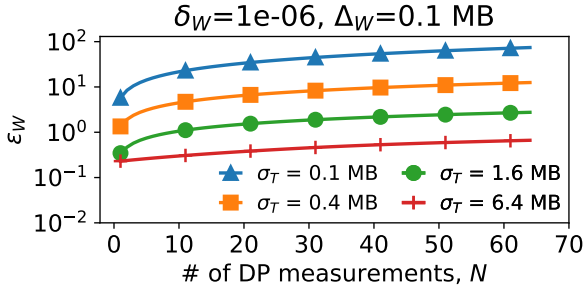


(d) Number of DP updates vs privacy loss

Figure 13: Per-window privacy loss $\varepsilon_W$ as a function of noise $\sigma_T$ (a, c), and number of DP measurements $N$ (b, d).

The probability that any attack can correctly identify the label for webpage $w_j$ is upper-bounded by:

$$\begin{aligned}&\Pr[A(T^D_{w_{i=j}}) = w_j]\\ &= \Pr[A(T^D_{w_{i=j}}) = w_j | T^D_{w_{i=j}} = T_{w_{i=j}}] \Pr[T^D_{w_{i=j}} = T_{w_{i=j}}] +\\ &\quad \Pr[A(T^D_{w_{i=j}}) = w_j | T^D_{w_{i=j}} = O_c] \Pr[T^D_{w_{i=j}} = O_c]\\ &\leq 1.(1-\beta) + \frac{1}{n}\beta = p^j_c\end{aligned}$$

For $(1-\frac{n\gamma-1}{n-1}) < \beta$ we have: $p^j_c \leq \gamma$.
Similarly, the probability that any attack can correctly classify $w_{i\neq j}$ is upper-bounded by $p^i_c = 1-\alpha+\frac{\alpha}{n}$, and for $(1-\frac{n\gamma-1}{n-1}) < \alpha$ we have: $p^j_c \leq \gamma$. Therefore, for all values of $\alpha$ and $\beta$ such that $(1-\frac{n\gamma-1}{n-1}) < \beta < \alpha$, the probability that any attack can successfully guess victim traffic stream in both cases is less than $\gamma$, and the defense is uniformly $\gamma$-private.
When the output of the algorithm is a constant pattern, $O_c$, with the probability $\beta$ the original webpage is $j$, and with probability $\alpha$, it can be any other webpages. Thus, we have:

$$\log(\frac{\Pr[T^D_{w_{i\neq j}} = O_c]}{\Pr[T^D_{w_{i=j}} = O_c]}) = \log(\frac{\alpha}{\beta}) > \varepsilon$$

Therefore, it fails to guarantee $\varepsilon$-differential privacy. □

**Lemma 2.** *A $\varepsilon$-differentially private shaping algorithm is Tamaraw $\gamma$-private for:*

$$\varepsilon \leq \log(n\gamma)$$

*Proof.* For a given trace, $w$, the random variable $T^{DP}_w$ represents packet trace of $w$ after a differentially private shaping mechanism is applied.
The classification attack on shaped traffic analysis the shaped traces so it can be considered as post-processing of the results of a differentially private shaping mechanism (i.e. defense), and is differentially private. Therefore, we have:

$$\frac{\Pr[A(T^{DP}_{w_i}) = w_i]}{\Pr[A(T^{DP}_{w_j}) = w_i]} \leq e^{\varepsilon}$$

$$\rightarrow \Pr[A(T^{DP}_{w_i}) = w_i] \leq e^{\varepsilon}.\Pr[A(T^{DP}_{w_j}) = w_i]$$

Intuitively, this implies that the likelihood of the attacker correctly classifying the trace with label $i$ compared to incorrectly classifying it with label $j$ is bounded by $e^{\varepsilon}$. The above inequality is correct for all $w_j : j \in \{1,2,\ldots,n\}$, therefore we can calculate the summation over $j$. Extending the above equation we have:

$$\begin{aligned}n \times \Pr[A(T^{DP}_{w_i}) = w_i] &\leq e^{\varepsilon} \sum_{j=1}^{n} \Pr[A(T^{DP}_{w_j}) = w_i]\\ &= e^{\varepsilon} \Pr_A[w_i]\end{aligned}$$

where $\Pr_A[w_i]$ is the probability that attack $A$ outputs the label $w_i$. Therefore, for any given trace $w_i$, the probability that any attack $A$, classifies it correctly is bounded by:

$$\Pr[A(T^{DP}_{w_i}) = w_i] \leq \frac{e^{\varepsilon} \Pr_A[w_i]}{n}$$

Therefore, the probability that an attacker can guess the vic-

tim's trace is bounded by:

$$\max_{w_i} \Pr[A(T^{DP}_{w_i}) = w_i] \leq \frac{e^{\varepsilon}}{n} \max_{w_i} \Pr_A[w_i] \leq \frac{e^{\varepsilon}}{n} \leq \gamma$$

□

Putting the two lemmas together, we prove that the notion of differential privacy is strictly stronger than Tamaraw's.